

Received 20 May 2022, accepted 22 June 2022, date of publication 7 July 2022, date of current version 19 July 2022.

Digital Object Identifier 10.1109/ACCESS.2022.3189017

RESEARCH ARTICLE

Intersection Complexity and Its Influence on Human Drivers

HANNES WEINREUTER¹, NADINE-REBECCA STRELAU², KEVIN QIU¹,
YANCHENG JIANG¹, BARBARA DEML², AND MICHAEL HEIZMANN¹

¹Institute of Industrial Information Technology (IIT)—Karlsruhe Institute of Technology (KIT), 76187 Karlsruhe, Germany

²Institute of Human and Industrial Engineering (ifab)—Karlsruhe Institute of Technology (KIT), 76131 Karlsruhe, Germany

Corresponding author: Hannes Weinreuter (hannes.weinreuter@kit.edu)

This work was supported by the Priority Program (“Schwerpunktprogramm” in German) 1835 “Cooperatively Interacting Automobiles” by the German Research Foundation (DFG).

This work involved human subjects or animals in its research. Approval of all ethical and experimental procedures and protocols was granted by the Ethics Commission of the KIT (in German: “Ethikkommission des KIT”).

ABSTRACT As mixed traffic between automated vehicles and human drivers in inner city becomes more prevalent in the near future understanding and predicting drivers’ behavior is important. Additionally, there is a wide variety of inner city intersections. They can differ greatly in traffic density, visibility, number of objects and many more aspects. This difference in complexity has an influence on the behavior of human drivers at intersections. To further understand the effect of complexity we conducted a naturalistic driving field study in inner city traffic with 34 participants. We focused on unsignalized intersections because there is a greater range of possibly ambiguous situations at such intersections than compared to e. g. an intersection regulated by traffic lights. Features describing the behavior (commit distance, drop in velocity and the minimal velocity) are extracted from the driven trajectories. Additionally, we define intersection complexity by several features describing an intersection. These features include both the static (street, visible and driveable width, the visibility of the other streets and the number of trees) and the dynamic environment (entry location and turning direction, numbers of vehicles, vehicles with interaction, vehicles with priority, vehicles having to yield and pedestrians). Based on those we show that the entry location and the turning direction have a significant effect on the behavior features. Additionally, we show that the typical behavior of human drivers can be predicted by the features describing an intersection’s complexity. Finally, the feature set is reduced in dimensionality for a more condensed intersection description. For that we test reduced feature sets as well as feature sets from an autoencoder and show that prediction is feasible with them as well.

INDEX TERMS Driving behavior prediction, intersection complexity, naturalistic driving, unsignalized intersection.

I. INTRODUCTION

The introduction of automated vehicles is a promising development for several reasons: It has the potential to be safer than human drivers, thus reducing the number and severity of accidents. It might also lead to better accessibility of mobility for people who are unable to drive themselves. However, there are still several challenges to overcome before automated

The associate editor coordinating the review of this manuscript and approving it for publication was Mauro Tucci¹.

vehicles can drive safely in any situation and environment. One of them is inner city traffic and especially mixed traffic consisting of both automated vehicles and vehicles driven by humans at unsignalized intersections.

This work focuses on the scenario of unsignalized intersections, i. e. intersections without traffic lights or priority signs to regulate traffic flow. This type of intersection is very common in Germany and other European countries in places where there is low to medium traffic. There the *right before left* rule applies. It states that a driver has priority

over vehicles coming from his/her left side and that a driver has to yield to vehicles coming from the right. Additionally, driving straight has priority over oncoming drivers turning left. As we assume no direct communication between vehicles, e. g. via *vehicle2vehicle* communication, drivers are required to interpret each other's intention and behavior and they have to communicate with each other. This is especially challenging for automated vehicles, as situations may arise that are not clearly defined or that have some ambiguity in the regulation. An example of that are deadlock scenarios in which every driver has to give way to at least one other driver. One way of dealing with this problem is to gain deeper knowledge of typical human behavior in such scenarios. Prior knowledge of typical behavior can be incorporated into the decision-making process of automated vehicles, since certain behaviors are more likely in a given circumstance. As this is an additional information source, decisions could be made more reliable. It might also allow for earlier decisions if the observed behavior matches the typical one. A deeper understanding of the typical behavior in these situations might also be of interest for intersection design to avoid collisions as there are traffic patterns at intersections that provide a potential for accidents.

For a deeper understanding of the driving behavior we look at the influence of intersection complexity on that. In this work the complexity of an intersection is described by features for both the static environment of an intersection (e. g. trees, the spatial surrounding like the visibility into the other roads and the driveable and perceived width of the street leading to an intersection) and the dynamic surroundings (e. g. pedestrians, the number of cooperation vehicles and the priorities according to traffic regulation). Additionally, we also consider the entry location and the turning direction through an intersection. The behavior of a driver is described by features derived from the driven trajectory. These include the distance at which a driver committed him-/herself to drive, the drop in velocity and the minimal velocity during the approach. Both the intersection and the behavior features are introduced in detail in section IV-A. To record the necessary data, we conducted a field study in which participants drove through inner city traffic while their driving behavior and data of the surrounding environment was recorded. Based on that data, we first investigate the influence of both the entry location and the turning direction on the driving behavior. We then use the complexity features of intersections to predict the driving behavior. Finally, several methods for dimensionality reduction are investigated to find a more condensed representation of the intersection complexity.

II. RELATED WORK

The focus of this work is on the influence of both the static and dynamic environment at an intersection on the behavior of drivers. External factors, both static (i. e. road infrastructure, buildings and vegetation) and dynamic (i. e. other traffic participants), have been investigated before in regard to their influence on driver behavior.



FIGURE 1. Test vehicle with sensor setup on the roof.

Many authors use features that describe static aspects of the driving environment in their work to define complexity. Imbsweiler *et al.* [1] argue, based on experimental results, that a T-junction can be considered as more complex than a narrow passage. A more general distinction between more and less complex environments has been used by Faure *et al.* [2] where an urban environment was seen as most complex, a rural road as medium and a highway section as least complex. Further external features for environmental complexity include the difference between signalized and unsignalized intersections [3] and the presence of parked vehicles on the street [4]. Wijnands *et al.* [5] analyzed intersection designs from satellite images. For that they define a complex intersection to have at least one multi-lane street, a slip lane, traffic islands or more than four legs. Comparing turning to driving straight through intersections is another aspect that can be considered [6], as well as visual clutter of traffic scenes [7].

It is reasonable to assume that besides the static environment of a traffic scene also dynamic aspects are influencing driving behavior and should thus be modeled as part of traffic complexity. Patten *et al.* [8] distinguish between three route complexity classes by assessing the demands on information processing and vehicle handling: A highly complex route has high demands in both categories. A medium complex route has high a demand in one category and a low demand in the other category. A route with a low complexity has low demands in either category. Jahn *et al.* [9] use the same definition but only the two extreme cases. Examples for high complexity are driving in an inner city or at signalized intersections where a driver has to give way. Medium complexity is assumed at signalized intersections with the right of way and at intersections regulated by traffic lights and low complexity is defined as situations where driving without interaction is possible [8], [9]. Further aspects of dynamic intersection features include traffic density and the occurrence of lane changes [10]. Manawadu *et al.* [11] manipulated complexity by varying the density of both vehicles and pedestrians at an intersection in a driving simulator. Lowest complexity in their work is the situation with both

the lowest density of pedestrians and vehicles, the highest complexity is assigned to the situation with the highest density of either parameter. Driving after a traffic congestion as compared to regular driving has been investigated as well [12]. For that a simulator study containing congested and non-congested intersections was conducted. Werneke and Vollrath [13] investigated the influence of traffic density and whether a zebra crossing was present at an intersection as part of intersection complexity.

Some authors also considered both static and dynamic influences: Oviedo-Trespalacios *et al.* [14] classify scenarios in an urban environment, car-following on suburban roads and driving on curved roads as complex. Cantin *et al.* [15] defined driving on a straight road as least complex. Their study also included intersections at which participants had to stop and an overtaking maneuver which they considered as most complex. Horberry *et al.* [16] varied environment complexity along a highway in a driving simulator by varying the number of billboards, buildings and other road infrastructure elements and the traffic density. In general one can conclude that there exists a wide variety of complexity definitions for road traffic. There is some consistency within them, most of those definitions do however only consider a small subset of all conceivable features that might contribute to the perceived complexity. Additionally, many of those definitions are either not specific to intersections or consider aspects of driving that are not related to intersections at all. In this work we intend to address this by using several features to describe intersection complexity.

Using the aspects of traffic environment complexity above, a wide range of influences on driver behavior has been investigated. Higher complexity has been shown to increase mental workload [2], [4], [6], [8]–[10], [14], [15]. Physiological parameters (electrocardiogram, electro-dermal activity, electroencephalography and gaze behavior) can be used to predict the perceived workload at intersections with varying complexity [11]. The influence of age and complexity on the driving behavior has also been of some interest [7], [15], [16]. Older drivers drive slower in more complex environments [16] and show increased workload compared to younger drivers in more complex driving contexts [15]. With increased visual clutter and age search efficiency for identifying traffic signs decreases [7]. There are differences in the visual scanning behavior while driving between signalized and unsignalized intersections [3]. Intersection complexity also has an influence on the driving behavior and the attention allocation [13]. When looking at deadlock situations drivers feel safer driving through the less complex symmetrical narrow passages than through T-intersections [1]. The driving behavior after a congestion is negatively influenced as it becomes more aggressive and drivers are less aware [12].

There exist several methods for assessing and quantizing driver behavior. A concept for which they are commonly used is the traffic conflict technique (TCT) [17]–[19]. The goal of the TCT is to assess traffic scenarios with regard to the conflicts occurring there and not only with data

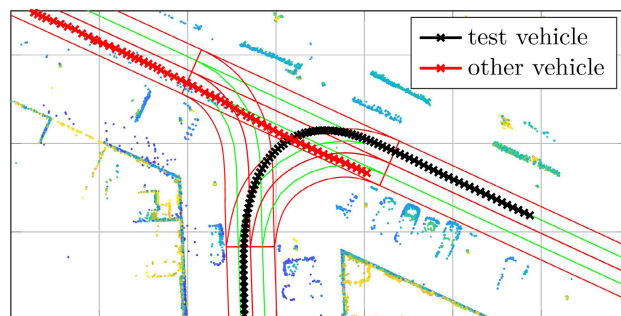


FIGURE 2. Top down view of a T-intersection with lanelets and tracks of the test vehicle (black) and one other car (red). Grid spacing: 10 m.

of actual accidents. A commonly used measure for driver behavior is the time to collision (TTC) [17]–[20]. Further behavior measures for drivers are the post-encroachment time (PET) [18] and the deceleration to safety (DST) [18], [19]. Minderhoud and Bovy [20] introduce extensions to the TTC concept to enable further and more detailed analyses. Domeyer *et al.* [19] employ TTC, PET, DTS and several other behavior features to investigate the interaction of drivers and pedestrians.

All these methods have in common that they investigate the interaction between drivers. As there are not necessarily other drivers present at the intersections in our work, we describe driving behavior differently by only considering the trajectory of the ego vehicle (cf. section IV-B). Features from only one vehicle have been used before, these include the velocity [4], [10], [12], [13], [16], the deviation from the speed limit [14], [16] and the lateral position on the lane [4], [10], [12]. Some of these authors also use variants such as mean, minimum and maximum values or the standard deviation.

There exist previous approaches to predict the intention and the behavior of human drivers in traffic. Several methods have been shown to be useful for that purpose. Streubel and Hoffmann [21] predict the driving path at a signalized intersection using a Hidden Markov Model (HMM). Long Short Term Memory (LSTM) Networks are also used to predict the turning direction [22], [23]. Ward and Folkesson [24] predict the driving behavior of drivers who have to yield at a signalized intersection. For that they apply k-Nearest Neighbors (k-NN), Support Vector Machines (SVM) and Random Forests (RF). From these methods we chose RF for this work.

III. DATA ACQUISITION

In order to obtain data of human behavior at inner city intersections, a field study was conducted. The driven trajectories of the participants were recorded and the passes through the relevant intersections were extracted for further analysis, as described in the following sections. The surroundings (i. e. traffic, buildings and vegetation) were recorded using a lidar sensor. All subjects were informed about the contents of the

study and signed a consent form prior to the experiment. The study was approved by the ethics commission of the KIT.

A. FIELD STUDY

The field study for this work was conducted in Karlsruhe, Germany. In total 34 participants (25 male, 8 female, one participant did not answer the questionnaire; average age: 27.9 a, $\sigma = 8.18$ a) drove a test vehicle on a predefined path in the inner city of Karlsruhe. An instructor seated in the rear of the vehicle guided the participants along the path. The course included 14 unsignalized T-shaped intersections and 4 unsignalized X-shaped intersections. As the intersections were unsignalized, the *right before left* rule applied. At one of the T-intersections participants were confronted with a deadlock situation that was generated by two additional vehicles driven by instructed drivers. At all remaining intersections the participants interacted with regular traffic. Four of the remaining intersections were specifically selected to include a wide range of traffic, both relatively close and distant surrounding buildings and different grades of overview over the intersection. The remaining intersections were not selected explicitly but were included as they were used to travel between the five selected intersections. The runs through the deadlock intersection are not subject of this work, the data set therefore contains the runs through the remaining 17 intersections. There are in total 1818 runs through the remaining 13 T-intersections and 565 runs through the 4 X-intersections in our data set. It took the participants on average 73.0 min ($\sigma = 6.4$ min) to complete the course of approximately 22 km.

The test vehicle that was used for this experiment is a commercially available *VW Passat* that is equipped with additional sensors and can be driven with a regular license. These sensors include a 16-channel lidar sensor with 600 RPM, an IMU with a sample rate of 400 Hz and two GPS receivers (1 Hz). Data is recorded using the Robotic Operating System (ROS) [25]. A picture of the vehicle is shown in Fig. 1.

B. TRAJECTORY GENERATION

The data from each participant was further processed to extract the driven trajectory of the test vehicle as well as the trajectories of surrounding vehicles the participant interacted with. For that a simultaneous localization and mapping (SLAM) approach [26] was applied to the measurement data to generate a precise track. The poses from the SLAM were then interpolated to 10 Hz to get a pose for each lidar revolution.

To cut the individual runs through the intersections from the global trajectories, all lidar revolutions were selected for a given run whose poses lay within a radius of 35 m from the intersection center. We used a simplified version of the lanelets concept [27], [28] for a comprehensive and accurate description of the intersections. These were created from map data. Our lanelets describe the polygon of a lane segment, its turning direction and the successor and predecessor lanelets,

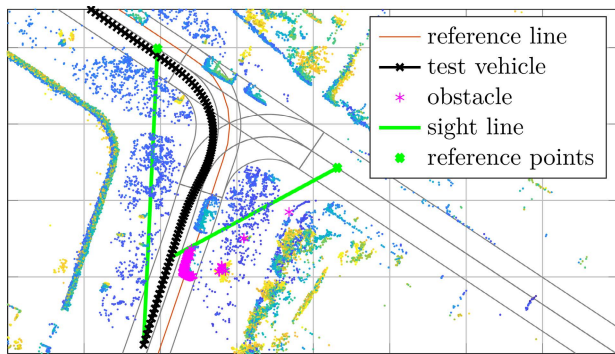
thus creating a lanelet graph. For each vehicle the most likely lanelet sequence is determined by considering the similarity of the direction of travel and the turning direction of the lanelet. If the distance between the trajectory and a lanelet sequence is too large, this sequence is taken out of consideration. Using the lanelet sequence a vehicle has driven along, the position from which it entered the intersection and the turning direction through the intersection (*left*, *right*, *straight*) can be inferred. To generate a consistent definition of the entry location (*left*, *right* and *bottom* for the T-junction; there is an additional *top* direction for X-intersections), all T-junctions were oriented to resemble the letter “T” and the labels were assigned accordingly. For the X-intersections the northernmost road was assigned the *top* label. Note that, depending on the entry location, not all turning directions are possible at a T-intersection. Both entry location and turning direction are used as features to describe intersection complexity in section V.

To detect moving objects within the lidar point clouds we use a clustering approach rather than a machine learning approach like PointNet [29] or PointPillars [30], since the lidar resolution is relatively low. The ground plane is removed using the matlab function `pcfitplane`. The point clouds are segmented into clusters where points of different clusters are at least $d_{\min} = 1.8$ m apart. Before clustering the point clouds are cut to include only those points above the lanelets. By doing so, we can make sure to only cluster objects, and therefore possible traffic participants, on the streets. We use an L-shape fitting method [31] to fit an accurate bounding box to each cluster. Bounding boxes that are implausibly large are removed. There is no minimum size requirement for a cluster.

A multi-object tracker using a global nearest neighbor assignment algorithm (`trackerGNN` function in Matlab) and an interacting motion model (IMM) tracking filter (`initekfimm` in Matlab) generate tracks from the cluster center points. The latter maintains three models of the objects with constant velocity, constant acceleration and constant turn. A multiple motion model is chosen since the road users are maneuvering, changing direction and speed. As road users are detectable for long periods of time and can be temporarily occluded, the tracker has to be set up to accommodate for that. When tracks are occluded, we interpolate linearly. Stationary tracks are removed and the velocity of the bounding boxes and their length and width are filtered with a median filter. The class of a moving object (pedestrian, cyclist, car and truck) is determined by the size and the speed of the clusters. In this work only two classes are used. Cyclists, cars and trucks are all considered as street based traffic participants. Pedestrians are viewed separately. An example of a run through a T-intersection is shown in Fig. 2. The test vehicle entered from the right and turned left. It had to interact with another traffic participant arriving from the left who was driving straight. The downsampled global point cloud is also shown, houses and some parked vehicles are visible.

TABLE 1. Features describing the intersection (top) and the driving behavior (bottom).

feature	description
p_e	position from which the intersection is entered (<i>left, right</i> or <i>bottom</i> , used only for T-intersections)
p_t	turning direction (<i>left, right</i> or <i>straight</i>)
n_p	number of detected pedestrians in scene
n_v	number of visible vehicles during approach
n_{vi}	number of interaction vehicles
n_{gw}	number of vehicles that had to give way
n_{rw}	number of vehicles that had the right of way
n_t	number of trees at intersection
d_{vr}	visibility distances based on the point clouds
d_{vp}	visibility distances based on object polygons
w_s	average width of street during approach
w_v	visual range during approach
w_a	available (driveable) street width during approach
v_{min}	minimal velocity during approach
v_d	relative drop in velocity during approach
d_c	commit distance: distance from intersection at which stopping in time is no longer possible

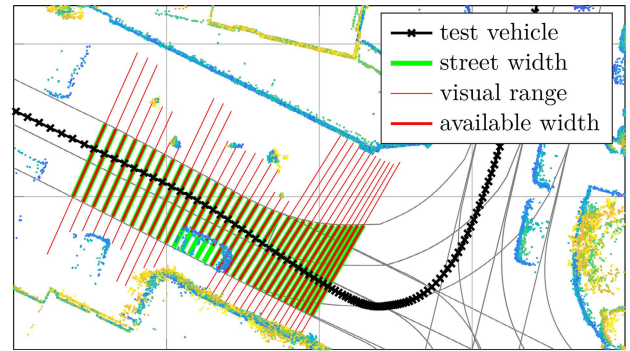
**FIGURE 3.** Visibility at a T-intersection. Test vehicle enters from the bottom and turns left. The reference point on the left street is visible from the start, the right street is blocked by parked cars, trees and a hedge. Grid spacing: 10 m.

IV. DATA PROCESSING

To investigate the behavior of human drivers at intersections, we need to be able to describe both the behavior of the drivers at an intersection and the intersection itself. For both we defined several features. An overview over all intersection and behavior features used in this work is given in table 1.

A. INTERSECTION FEATURES

The intersections are represented by features that describe the traffic and features characterizing the geometry of the intersection. Both are included here as we assume that both have an influence on the complexity perceived by a human driver. The number of pedestrians n_p includes all pedestrians that have been identified in the lidar data from a run through the intersection. Identified vehicles are counted in n_v . Both pedestrians and vehicles are counted if they are visible during the approach, i. e. their track has to start before the distance to the intersection of the ego vehicle is zero. To distinguish between all visible vehicles and the ones relevant for the par-

**FIGURE 4.** Street width, visual range and available width from 25 m to 7 m before the intersection center. The test vehicle enters from the left side and turns left. Grid spacing: 10 m.

ticipant, the number of interaction vehicles n_{vi} are counted as well. These vehicles were within 10 m from the intersection center at the same time as the test vehicle and were observed to pass the intersection center. These vehicles are further analyzed as to whether they have to give way to the test vehicle (n_{gw}) or if they have the right of way themselves (n_{rw}). As we are only investigating unsignalized intersections the priority is determined by investigating the relative directions from which two vehicles enter the intersection and the directions of travel through the intersection. The analysis is performed pairwise and includes all pairs the test vehicle is a part of. If for example a vehicle turns left, it has to yield to a vehicle entering from straight ahead and driving straight through the intersection. We assume that more traffic contributes to the perceived complexity as there are more possible cooperation partners a driver has to interact with and more information has to be processed to resolve a situation.

The spatial properties of an intersection are described with two concepts, the width and the visibility distance. Additionally, the number of trees n_t near the intersection and along the driven street is used as a feature. The visibility at an intersection is described by the distance from the intersection center at which reference points are visible. It is assumed relevant because if a cooperation partner is visible earlier there is more time left to react to a given situation. The visibility distance is calculated by two methods, using a ray-tracing approach or by a polygon based approach. For both versions reference points $\mathbf{p}_{ref,i}$ are placed on the streets of the intersection other than the one the vehicle approached the intersection from. There are therefore two reference points at a T-intersection and three at X-intersections. Of these points, those on the street straight ahead are omitted, as it is always visible at all intersections in our data set during the approach. One or two reference points remain in the case of a T-junction, as there is no street straight ahead when approaching from the bottom. At X-intersections there are always two points remaining. The use of the reference points is showcased in Figure 3. The vehicle approaches from below. As there is no top street at a T-intersections, the reference points on both the left and right

street remain. The reference points are placed in the center of their road at a distance from the intersection center where a car driving at the speed limit ($v_{\max} = 30 \text{ km h}^{-1}$) can stop from at the intersection center:

$$d_{\text{ref}} = v_{\max} \cdot t_r + \frac{v_{\max}^2}{2 \cdot |a_b|}. \quad (1)$$

The calculation is based on the reaction time $t_r = 1 \text{ s}$ and the breaking deceleration $a_b = -6 \text{ m s}^{-2}$. These values result in $d_{\text{ref}} = 14.12 \text{ m}$. In the following all distances are measured along the center line of the concatenated lanelet sequence the test vehicle drove on. For that the start and the end point of the distance to be measured are projected onto the center line of the lanelet sequence.

For the ray-tracing approach, the two lidar scans before and the two scans after are merged with the current scan to a merged point cloud $\mathbf{P}_m(d) = [\mathbf{x}, \mathbf{y}, \mathbf{z}]$, where d is the distance along the lane center line to the intersection center. A sight line 1 m above ground from the current location to every reference point is created: $s_i(d) = [\mathbf{x}(d), \mathbf{p}_{\text{ref},i}]$. If there is no point of $\mathbf{P}_m(d)$ within a cylinder $C_{s,i}(d)$ of radius 0.6 m along $s_i(d)$, this reference point is considered visible from the current distance. The visibility distance for reference point i is then the maximum distance from which it is visible:

$$d_{\text{vr},i} = \arg \max_d (C_{s,i}(d) \cap \mathbf{P}_m = \emptyset). \quad (2)$$

The calculation is showcased in Fig. 3. Alternatively, the visibility can also be calculated by only taking stationary objects into consideration. For that we do not rely on the recorded point clouds, instead polygon sets of buildings P_b and trees P_t were generated for each intersection. If the sight line of reference point i does not intersect with any polygon, the reference point is considered visible:

$$d_{\text{vp},i} = \arg \max_d (P_b \cap P_t \cap s_i(d) = \emptyset). \quad (3)$$

The visibility distance for a given intersection is the minimal visibility distance over all its streets:

$$d_{\text{vx}} = \min_i(d_{\text{vx},i}). \quad (4)$$

To measure the narrowness of the street leading up to an intersection, we define three widths. The widths are measured along the normal $\mathbf{n}_s(d)$ to the driven trajectory parallel to the ground plane. The width of the street includes the opposite lane. For that reason the two intersections to the left $\mathbf{p}_{s,l}(d)$ and right $\mathbf{p}_{s,r}(d)$ of $\mathbf{n}_s(d)$ with the street polygon created from the lanelets are calculated. The street width $w_s(d)$ is the Euclidean distance between the two intersection points:

$$w_s(d) = |\mathbf{p}_{s,l}(d) - \mathbf{p}_{s,r}(d)|_2. \quad (5)$$

The visual range describes how far a driver can see to the left and right. The view is usually blocked by parked vehicles, other traffic participants, signs, vegetation or buildings. Some of the objects and obstacles that are considered here are also considered by other features like the number of trees n_t . It is calculated along the normal at sensor height $\mathbf{n}_v(d)$. The first

points within $\pm 10 \text{ deg}$ in horizontal direction and $\pm 5 \text{ deg}$ in vertical direction to the left ($\mathbf{p}_{v,l}(d)$) and to the right ($\mathbf{p}_{v,r}(d)$) determine the limits of the visual range:

$$w_v(d) = |\mathbf{p}_{v,l}(d) - \mathbf{p}_{v,r}(d)|_2. \quad (6)$$

The available street width represents the width of the street that is vacant and available to the driver:

$$w_a(d) = \min(w_s(d), w_{v,\text{mod}}(d)). \quad (7)$$

The visual range $w_v(d)$ is modified to include a vertical range of $\pm 15 \text{ deg}$. All three widths are averaged from 25 m to 7 m before the intersection center. The difference between the three widths is visualized in Fig. 4. The widths are included to represent both the available space for driving (street width and available width) and the perceived narrowness of a situation (visible width) in the feature set. Less space might increase the perceived complexity of a situation.

It should be noted that the features describing the intersection are used as a surrogate for the overall intersection complexity perceived by a human driver and are assumed to describe the complexity of an intersection. The selection of features is based both on features found in literature and on the authors' considerations. A subjective rating of complexity for the intersections could not be recorded reliably in this study.

B. BEHAVIOR FEATURES

Besides the features that describe the intersection and the traffic, we additionally need features that describe the driving behavior of the participants of the study. For that selection, several aspects have to be considered: These features have to be applicable to situations with and without cooperation partners. Additionally, the intersections that were included in the study have several attributes in common: The speed limit is always 30 km h^{-1} , there is one lane per street and direction and all intersections are located within residential areas. Finally, typical aspects of driving at intersections have to be described by them.

In this work we use three features to describe the behavior of human drivers at an intersection: The minimum velocity, the velocity drop during the approach and the commit distance. The features are calculated from the driven trajectory of the test vehicle. All features are based on the approach interval from $d_s = 25 \text{ m}$ from the intersection center to $d_e = 0 \text{ m}$. This interval starts at a distance shortly before a majority of drivers started changing their velocity and ends at the intersection center. The minimum velocity is the lowest velocity during the approach:

$$v_{\min} = \min(v(d)), \quad d_s > d > d_e. \quad (8)$$

The second feature is the velocity drop during the approach to an intersection:

$$v_d = \frac{v_{\min}}{v_a}, \quad (9)$$

with the mean initial approach velocity v_a in the interval from 25 m to 20 m from the intersection. The final feature

TABLE 2. Mean of behavior at T-intersections, standard deviation in brackets.

	entry location			turning direction		
	bottom	left	right	left	right	straight
commit dist. in m	3.29 (1.37)	7.07 (2.38)	7.85 (3.56)	3.93 (1.79)	5.60 (1.48)	9.47 (2.98)
min. velocity in m s^{-1}	2.11 (1.32)	4.60 (1.42)	4.95 (2.06)	2.53 (1.55)	3.94 (0.98)	5.73 (1.84)
velocity drop	0.36 (0.22)	0.72 (0.20)	0.73 (0.23)	0.41 (0.24)	0.62 (0.16)	0.85 (0.20)

is the commit distance d_c . It describes the distance to the intersection center at which, given the current velocity, the test vehicle cannot stop in time anymore:

$$d_c = \max_d \left(d < v(d) \cdot t_r + \frac{v(d)^2}{2|a_b|} \right). \quad (10)$$

We found that these features meet the requirements from above and are well suited for behavior prediction. Minimum velocity and the velocity drop describe the breaking behavior at an intersection, the commit distance can be seen as an indicator of where a decision on the driving behavior has been made. There are several more possible behavior features that could be used here like velocity, acceleration or the distance to the intersection center where the minimal velocity is reached. In this work, however, we focused on those three as an example.

V. ANALYSIS

Using the intersection complexity, in the form of the features derived from the data set, several aspects are analyzed. First, we investigate how the driving behavior is dependent on the entry location and turning direction at intersections. Additionally, we look at how the features that constitute the intersection complexity influence a driver's behavior and how to predict it. We finally investigate several lower dimensional representations of intersection complexity. For all variants the behavior features from the previous section are used.

A. INFLUENCE OF ENTRY LOCATION AND TURNING DIRECTION ON THE DRIVING BEHAVIOR

First we analyzed the drivers' behavior depending on where they entered or how they drove through the intersection. For both intersection types the turning direction (*left*, *right* or *straight*) has to be considered. Depending on the direction drivers might have the right of way or have to give way and therefore show different behavior. For the T-intersection the entry location (*left*, *right* or *bottom*) also has to be considered as different traffic constellations can occur and visibility differs between entry locations. As the X-intersection is symmetrical the entry location can be neglected.

For analysis, ANOVAs on mixed linear-models were calculated using *R* in version 4.0.4 with the package *lmerTest* [32]. Normal distribution was not given for neither the X-intersection nor the T-intersection, but studies show

TABLE 3. Mean of behavior at X-intersections, standard deviation in brackets.

	turning direction		
	left	right	straight
commit dist. in m	3.19 (0.81)	4.95 (1.65)	8.16 (3.46)
min. velocity in m s^{-1}	1.88 (0.98)	3.48 (1.12)	5.03 (2.20)
velocity drop	0.32 (0.17)	0.56 (0.17)	0.76 (0.25)

that linear mixed-models are robust against violations of normal distribution [33], [34]. For the X-intersection linear models with turning directions as predictor were calculated, for the T-intersection turning direction and entry location were used as predictors. Mean and standard deviation for commit distance, minimal speed and relative speed drop at the T-intersections can be found in table 2 and at the X-intersections in table 3.

For both the X-intersections ($F(2, 532.02) = 153.47$, $p < .001$) as well as the T-intersections ($F(2, 1780.9) = 917.05$, $p < .001$), the turning direction shows a significant effect on the commit distance. Bonferroni corrected post-hoc tests revealed a significant difference between all the turning directions for the X-intersections as well as for the T-intersections ($p < .001$). For the T-intersections the entry location also showed a significant effect on the commit distance ($F(2, 1780.6) = 446.76$, $p < .001$). The commit distance was significantly lower when entering from the bottom of the intersection compared to the left ($p = .032$) or the right ($p < .001$). The commit distance from the right was significantly higher than that from the left ($p < .001$).

The minimal speed while approaching the intersection differed significantly between turning direction at the X-intersections ($F(2, 531.86) = 119.12$, $p < .001$) as well as at the T-intersections ($F(2, 1780.9) = 473.15$, $p < .001$). Post-hoc tests showed that at the X-intersections minimal speed was significantly higher when driving straight compared to left ($p < .001$) or right ($p < .001$) and when driving right compared to left ($p < .001$). The same pattern could be observed for the T-intersections ($p < .001$ respectively). Entry location at the T-intersections also has a significant effect on the minimal speed ($F(2, 1780.6) = 366.60$, $p < .001$). Minimal speed was significantly lower when entering from the bottom compared to left ($p < .001$) or right ($p < .001$) as well when comparing left to right ($p < .001$).

The relative speed drop is significantly different between turning directions for the X-intersections ($F(2, 531.74) = 140.47$, $p < .001$) as well as the T-intersections ($F(2, 1781.0) = 342.28$, $p < .001$). Post-hoc tests showed that the relative speed drop is significantly higher when driving straight compared to left or right and driving right compared to left for both types of intersection ($p < .001$ respectively). The entry location at the T-intersections also has a significant effect on the relative speed drop ($F(2, 1780.6) = 272.66$, $p < .001$). It is significantly higher when entering from the right compared to left

TABLE 4. Regression parameters for the T-intersection models for all behavior features. $p < .001$ for all entries but the one marked with an asterisk which has a value of $p = .011$.

	commit dist.		min. velocity		velocity drop	
	b	SE	b	SE	b	SE
intercept	2.86	0.12	1.796	0.08	0.32	0.01
entry loc. left	0.35*	0.14	0.45	0.10	0.11	0.01
entry loc. right	3.14	0.11	2.14	0.08	0.28	0.01
turning dir. right	2.49	0.14	1.80	0.10	0.22	0.01
turning dir. straight	5.53	0.14	3.04	0.10	0.38	0.01

TABLE 5. Regression parameters for the X-intersection models for all behavior features. $p < .001$ for all entries.

	commit dist.		min. velocity		velocity drop	
	b	SE	b	SE	b	SE
intercept	3.19	0.33	1.89	0.22	0.32	0.03
turning dir. right	1.76	0.36	1.59	0.23	0.24	0.03
turning dir. straight	4.97	0.35	3.15	0.23	0.44	0.03

($p < .001$) or bottom ($p < .001$) and left compared to bottom ($p < .001$). The regression parameters for these models are listed in Table 4 for the T-intersection models and in Table 5 for the X-intersection models.

From these results we can see that both the turning direction at and the entry location into T-intersections have a significant influence on the typical behavior of drivers. This information is therefore useful when designing decision-making algorithms for these scenarios. The fact that the commit distance is smaller, the minimum velocity is lower and that the velocity drop is more pronounced when entering from the bottom road indicates that drivers tend to approach an intersection more cautiously from the bottom and make their final decision closer to the intersection in this case.

B. BEHAVIOR PREDICTION BASED ON INTERSECTION COMPLEXITY

To evaluate if the complexity of an intersection has any influence on the behavior of human drivers, random forest [35], [36] regression has been applied to predict the behavior based on the features from section IV-A describing the intersections. RFs can be used for both, classification and regression and have been applied to many different fields, e. g. classifying drivers' intentions at intersections [24], as part of a system for link fault identification in networks [37] or for capacity estimation of lithium-ion batteries [38]. There are many more methods that could be used for regression here as well. The goal of this work is to showcase that predicting driving behavior based on intersection complexity features is possible. RFs are a good fit for that as they allow to model non-linear dependencies [36] and for their ease of use. For all cases in our work an RF regression model with 300 trees is trained. In the remainder of this paper the term *regression* refers to the Random Forest regression. In a first step all 11 intersection features from section IV-A were used. These are the number of pedestrians n_p , the number of visible vehicles n_v , the

number of vehicles that the participant interacted with n_{vi} , the number of vehicles that had to give way n_{gw} and those which had the right of way n_{rw} . The number of trees n_t , the visibility distances based on the point clouds d_{vr} and on the object polygons d_{vp} , the street width w_s , the visual range w_v and the available street width w_a are also included. Since the turning direction p_t and in the case of the T-intersection also the entry location p_e have a significant influence on the behavior of drivers, they were also added to the feature set describing the intersection complexity. Both the T- and the X-intersection data set were split into a training and a test set, the two intersection types were analyzed separately. The test sets contained 30 % of all runs through the intersections. The training sets were used to train the RF regression models. All evaluations were performed on the test set and the Root Mean Squared Error (RMSE)

$$\text{RMSE} = \sqrt{\frac{1}{N} \sum_{k=1}^N (\hat{y}_k - y_k)^2} \quad (11)$$

and the Mean Absolute Error (MAE)

$$\text{MAE} = \frac{1}{N} \sum_{k=1}^N |\hat{y}_k - y_k|_2 \quad (12)$$

of the regression results are calculated for that, with N being the number of test samples, y_k the behavior feature as extracted from the k -th member of the test set and \hat{y}_k the estimated behavior feature from the regression for the k -th member of the test set. The results are given in the first line of Table 6 for the T-intersections and in Table 7 for the X-intersections. All values in these tables are calculated by running the RF regression ten times with different training and test set assignments. The values shown are the average over the test results of all iterations. Additionally, in the last line of the tables the reference values are given. These values are the results of a naive classifier that outputs the mean of the training set. The scatter plots of the best of the ten runs of the RF regression are shown in Figure 5a for the data of the T-intersections and in Figure 5b for the X-intersections.

The scatter plots show that there are few outliers, most test examples are predicted relatively close to the ideal line. For both intersection types, it is noteworthy that the regression of the minimum velocity and the velocity drop are unreliable where the vehicle is very slow or even stopped. For all features the behavior can be predicted reliably using the complexity features, especially considering that the driving style and behavior might be influenced by other factors such as the driver's personality. Similar results can be obtained using other behavior features like velocity or acceleration.

C. BEHAVIOR PREDICTION WITH LOWER DIMENSIONAL COMPLEXITY

As we are ideally interested in a one-dimensional intersection description (i. e. the complexity of an intersection), an analysis whether a reduction of the complexity feature set is feasible was conducted. As there are several features in the data set

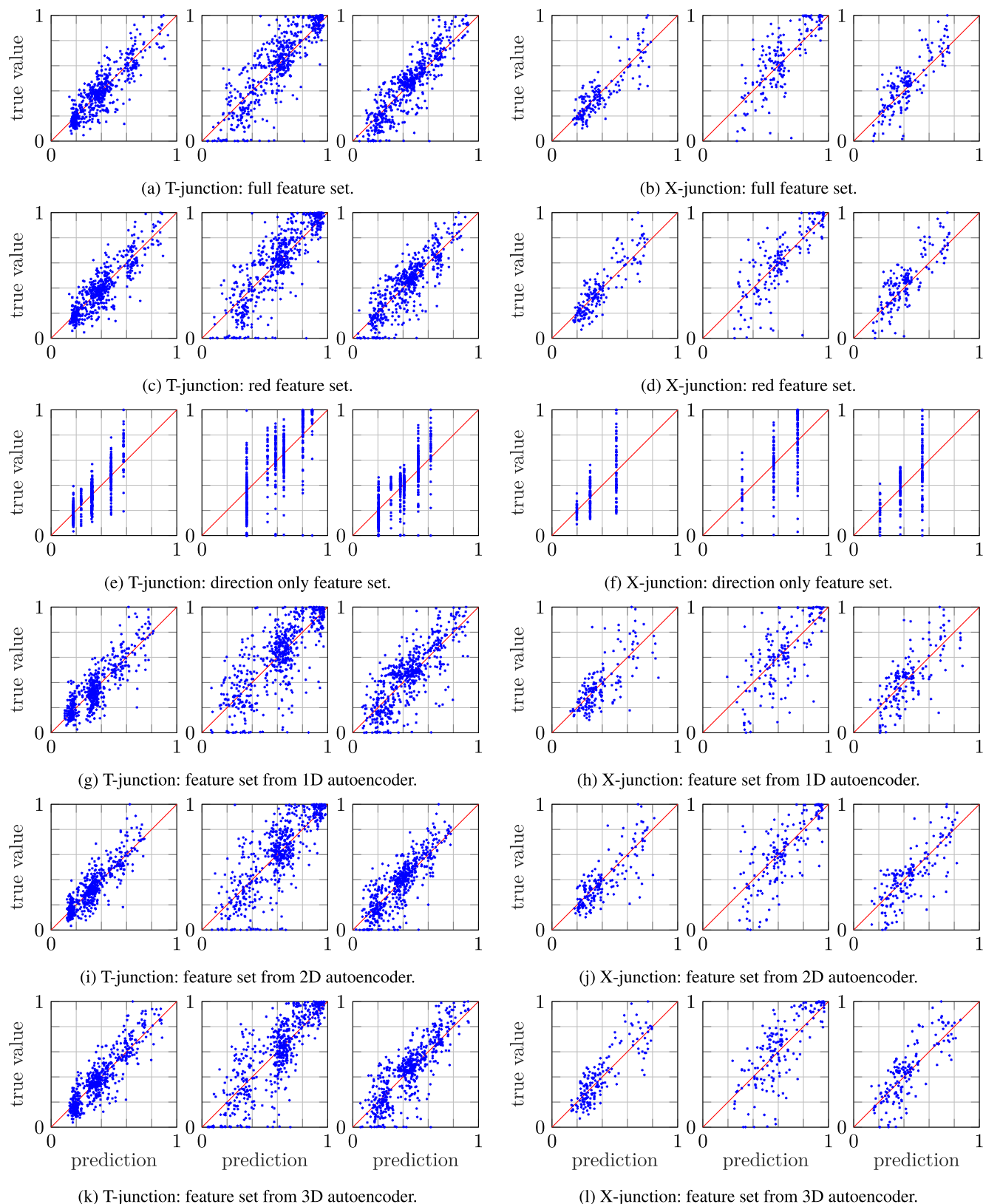


FIGURE 5. Normalized regression results on the test set data of the best performing regression using different feature sets.

that are defined similarly, initially a reduction of the features to only include the most relevant ones was performed. The

resulting reduced feature set is a compromise between the feature importance of all six RF regressions with the full

TABLE 6. Mean regression results for T-intersection using different feature sets (FS) and all behavior features: commit distance d_c , minimum velocity v_{\min} and velocity drop v_d . Standard deviation in brackets.

	d_c in m		v_{\min} in m s^{-1}		v_d	
	RMSE	MAE	RMSE	MAE	RMSE	MAE
full FS	1.492 (0.050)	1.095 (0.049)	1.033 (0.036)	0.750 (0.028)	0.153 (0.005)	0.111 (0.003)
red. FS	1.512 (0.049)	1.108 (0.048)	1.068 (0.036)	0.775 (0.028)	0.157 (0.006)	0.114 (0.003)
dir. FS	1.800 (0.068)	1.333 (0.052)	1.298 (0.041)	0.973 (0.037)	0.187 (0.006)	0.142 (0.004)
AE 1D	1.838 (0.121)	1.338 (0.084)	1.317 (0.034)	0.966 (0.022)	0.189 (0.006)	0.137 (0.005)
AE 2D	1.647 (0.082)	1.209 (0.065)	1.185 (0.039)	0.867 (0.031)	0.174 (0.005)	0.125 (0.003)
AE 3D	1.617 (0.067)	1.186 (0.044)	1.165 (0.047)	0.847 (0.028)	0.170 (0.008)	0.123 (0.004)
ref.	3.093 (0.116)	2.408 (0.075)	1.977 (0.051)	1.547 (0.044)	0.275 (0.004)	0.226 (0.005)

TABLE 7. Mean regression results for X-intersection using different feature sets (FS) and all behavior features: commit distance d_c , minimum velocity v_{\min} and velocity drop v_d . Standard deviation in brackets.

	d_c in m		v_{\min} in m s^{-1}		v_d	
	RMSE	MAE	RMSE	MAE	RMSE	MAE
full FS	1.696 (0.093)	1.279 (0.061)	1.150 (0.057)	0.862 (0.042)	0.159 (0.008)	0.118 (0.005)
red. FS	1.728 (0.110)	1.294 (0.071)	1.173 (0.069)	0.874 (0.043)	0.162 (0.008)	0.118 (0.006)
dir. FS	2.590 (0.084)	1.990 (0.080)	1.686 (0.045)	1.296 (0.041)	0.209 (0.008)	0.161 (0.005)
AE 1D	2.515 (0.267)	1.859 (0.186)	1.625 (0.186)	1.232 (0.127)	0.212 (0.020)	0.161 (0.014)
AE 2D	2.092 (0.174)	1.561 (0.152)	1.371 (0.108)	1.042 (0.100)	0.186 (0.013)	0.139 (0.011)
AE 3D	1.999 (0.170)	1.519 (0.124)	1.323 (0.095)	1.004 (0.067)	0.179 (0.007)	0.135 (0.006)
ref.	3.229 (0.135)	2.519 (0.123)	2.000 (0.075)	1.537 (0.079)	0.256 (0.011)	0.210 (0.010)

data set and was generated empirically. The turning direction p_t and, in the case of the T-intersection, the entry location p_e , the visibility distances based on ray-tracing d_{vr} and the polygons d_{vp} , the available width w_a , the street width w_s , the number of trees n_t and the number of visible vehicles n_v were most important. All features but n_v describe the static environment of an intersection, the only feature describing the traffic that was included in the reduced set is the number of visible vehicles n_v . This does not necessarily mean that the dynamic environment is less important for the behavior at an intersection. As we were driving through normal traffic, most runs through the intersections happened without any interaction partners, thus reducing their overall influence on the behavior in our data set. The RF regression results using the reduced feature set are shown in the second row of Table 6 and Table 7, respectively. The scatter plots are given in Figure 5c and Figure 5d.

The results of the reduced feature set are very similar to those of the full set. All features are predicted less accurately, the difference is more pronounced in the case of the X-intersection. The high importance of those features describing stationary aspects of an intersection indicates that the desired path through an intersection and the intersection

itself are important factors affecting the behavior at and thus the complexity of an intersection. The relatively low influence of features describing the traffic might in part be influenced by the fact that there was no additional traffic other than the test vehicle in several runs.

In section V-A we showed that the entry location p_e and turning direction p_t are important factors to the behavior of a driver at an intersection. We therefore reduced the feature set further so that it only included the turning direction and additionally the entry location in the case of the T-intersections. The results are given in the third line of Table 6 and Table 7. The results are worse than those of both the full and the reduced feature sets; this is especially the case for the X-intersections. One likely cause for the reduced accuracy is the limited set of possible values of these features. In the case of the T-intersections there are only six possible values for the direction features, for the X-intersections this is further reduced to three values. The regression can only assume at most as many distinct values as there are possible combinations of feature values. This can also be seen in the scatter plots for these feature sets in Figure 5e and Figure 5f. Considering that the performance of the regression is reduced but still considerably better than the reference we can again conclude that the entry location and the turning direction are important features for predicting the driving behavior.

Finally, an autoencoder (AE) was used to reduce the dimensionality of the complexity feature set describing the intersections. For that purpose an AE was trained to generate a low-dimensional representation of the full feature set. An AE is a special form of neural network that can be used to generate a lower dimensional, non-linear representation of a given feature space [39]. For these reasons and the ability to include categorical data we chose an AE over e. g. principal component analysis (PCA). An AE consists of an encoder and a decoder, the number of neurons is typically lower at the interface between the two [39]. The dimension at this bottleneck of the AE was set to either $d_{AE} = \{1, 2, 3\}$. The representation of the complexity features at the bottleneck was then used to train the RF regression as before. To train the AE 50 % of the data set was used as the training set and 20 % as the validation set. The RF regression was then trained with the compressed representation of the features of both the training and the validation set. The results were again obtained by analyzing the test set. Both the encoder and the decoder consist of three layers. All layers are fully connected layers with ReLU and batch normalization after each layer. The input dimension of the encoder is determined by the dimensionality of the full feature set (17 for the T-intersection and 14 for the X-intersection; the categorical features are one-hot encoded). The dimension at the output of the encoder is determined by d_{AE} and the intermediate layers have the dimension 15 and 6, respectively. The decoder is set up in reverse. For each direction feature cross entropy (CE) is used as the loss function while the loss of the remaining features is calculated using the mean squared error (MSE). The total loss is the weighted sum of the partial losses. The results of the RF

regression based on the AE latent representations are given in Table 6 and Table 7, the scatter plots for the 1D case are shown in Figure 5g and Figure 5h, for the 2D case in Figure 5i and Figure 5j and for the 3D case in Figure 5k and Figure 5l.

These results show that behavior prediction is also feasible with a low dimensional representation of the intersection complexity features. It is noteworthy however that the results for the 1D case are comparable to the case of the entry location and turning direction only feature set. For the 2D and 3D case the performance is improved compared to the 1D case but still worse than in the cases of the full or reduced data sets. This is especially the case for the X-intersections.

VI. CONCLUSION

In this work a data set with runs through unsignalized inner city intersections was recorded. Based on that data set the factors that influence the complexity of an intersection were analyzed. The results show that the desired turning direction through an intersection has a significant influence on the behavior of a human driver. At T-intersections the entry location also significantly influences the behavior. Additionally, we showed that the behavior can be predicted by an RF regression based on features describing the complexity of an intersection. Besides, a reduction of the feature set and a dimensionality reduction using an AE were performed. These feature sets proved suitable for behavior prediction with RF regression as well.

To understand and reliably predict human driving behavior at intersections the turning direction and entry location as well as static and dynamic features of the intersection environment have to be considered. This knowledge can be beneficial in decision-making models for example. Here it could be used as prior knowledge to take typical behavior of human interaction partners into account depending on the complexity.

In future work we plan to also assess the perceived complexity of the intersection by human drivers through further studies. With that we intend to gain a deeper understanding of the correlations between the perceived complexity and the multidimensional representation of complexity through features of intersections used in this work. These results could then be incorporated into an algorithm for automated vehicles driving through unsignalized intersections in mixed traffic.

ACKNOWLEDGMENT

Mapping data has been provided by the City of Karlsruhe.

REFERENCES

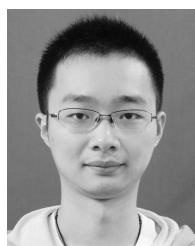
- [1] J. Imbsweiler, M. Ruesch, H. Weinreuter, F. Puente León, and B. Deml, "Cooperation behaviour of road users in t-intersections during deadlock situations," *Transp. Res. F, Traffic Psychol. Behav.*, vol. 58, pp. 665–677, Oct. 2018.
- [2] V. Faure, R. Lobjois, and N. Benguigui, "The effects of driving environment complexity and dual tasking on drivers' mental workload and eye blink behavior," *Transp. Res. F, Traffic Psychol. Behav.*, vol. 40, pp. 78–90, Jul. 2016.
- [3] G. Li, Y. Wang, F. Zhu, X. Sui, N. Wang, X. Qu, and P. Green, "Drivers' visual scanning behavior at signalized and unsignalized intersections: A naturalistic driving study in China," *J. Saf. Res.*, vol. 71, pp. 219–229, Dec. 2019.
- [4] J. Edquist, C. M. Rudin-Brown, and M. G. Lenné, "The effects of on-street parking and road environment visual complexity on travel speed and reaction time," *Accident Anal. Prevention*, vol. 45, pp. 759–765, Mar. 2012.
- [5] J. S. Wijnands, H. Zhao, K. A. Nice, J. Thompson, K. Scully, J. Guo, and M. Stevenson, "Identifying safe intersection design through unsupervised feature extraction from satellite imagery," *Comput.-Aided Civil Infrastruct. Eng.*, vol. 36, no. 3, pp. 346–361, Mar. 2021.
- [6] P. A. Hancock, G. Wulf, D. Thom, and P. Fassnacht, "Driver workload during differing driving maneuvers," *Accident Anal. Prevention*, vol. 22, no. 3, pp. 281–290, Jun. 1990.
- [7] G. Ho, C. T. Scialfa, J. K. Caird, and T. Graw, "Visual search for traffic signs: The effects of clutter, luminance, and aging," *Hum. Factors, J. Hum. Factors Ergonom. Soc.*, vol. 43, no. 2, pp. 194–207, Jun. 2001.
- [8] C. J. D. Patten, A. Kircher, J. Östlund, L. Nilsson, and O. Svenson, "Driver experience and cognitive workload in different traffic environments," *Accident Anal. Prevention*, vol. 38, no. 5, pp. 887–894, Sep. 2006.
- [9] G. Jahn, A. Oehme, J. F. Krems, and C. Gelau, "Peripheral detection as a workload measure in driving: Effects of traffic complexity and route guidance system use in a driving study," *Transp. Res. F, Traffic Psychol. Behav.*, vol. 8, no. 3, pp. 255–275, May 2005.
- [10] E. Teh, S. Jamson, O. Carsten, and H. Jamson, "Temporal fluctuations in driving demand: The effect of traffic complexity on subjective measures of workload and driving performance," *Transp. Res. F, Traffic Psychol. Behav.*, vol. 22, pp. 207–217, Jan. 2014.
- [11] U. E. Manawadu, T. Kawano, S. Murata, M. Kamezaki, J. Muramatsu, and S. Sugano, "Multiclass classification of driver perceived workload using long short-term memory based recurrent neural network," in *Proc. IEEE Intell. Vehicles Symp. (IV)*, Jun. 2018, pp. 1–6.
- [12] G. Li, W. Lai, X. Sui, X. Li, X. Qu, T. Zhang, and Y. Li, "Influence of traffic congestion on driver behavior in post-congestion driving," *Accident Anal. Prevention*, vol. 141, Jun. 2020, Art. no. 105508.
- [13] J. Werneke and M. Vollrath, "What does the driver look at? The influence of intersection characteristics on attention allocation and driving behavior," *Accident Anal. Prevention*, vol. 45, pp. 610–619, Mar. 2012.
- [14] O. Oviedo-Trespalacios, M. M. Haque, M. King, and S. Washington, "Effects of road infrastructure and traffic complexity in speed adaptation behaviour of distracted drivers," *Accident Anal. Prevention*, vol. 101, pp. 67–77, Apr. 2017.
- [15] V. Cantin, M. Lavallière, M. Simoneau, and N. Teasdale, "Mental workload when driving in a simulator: Effects of age and driving complexity," *Accident Anal. Prevention*, vol. 41, no. 4, pp. 763–771, Jul. 2009.
- [16] T. Horberry, J. Anderson, M. A. Regan, T. J. Triggs, and J. Brown, "Driver distraction: The effects of concurrent in-vehicle tasks, road environment complexity and age on driving performance," *Accident Anal. Prevention*, vol. 38, no. 1, pp. 185–191, Jan. 2006.
- [17] H.-C. Chin and S.-T. Quek, "Measurement of traffic conflicts," *Saf. Sci.*, vol. 26, no. 3, pp. 169–185, Aug. 1997.
- [18] C. Johnsson, A. Laureshyn, and T. De Ceunynck, "In search of surrogate safety indicators for vulnerable road users: A review of surrogate safety indicators," *Transp. Res.*, vol. 38, no. 6, pp. 765–785, Nov. 2018.
- [19] J. E. Domeyer, J. D. Lee, H. Toyoda, B. Mehler, and B. Reimer, "Interdependence in vehicle-pedestrian encounters and its implications for vehicle automation," *IEEE Trans. Intell. Transp. Syst.*, vol. 23, no. 5, pp. 4122–4134, May 2022.
- [20] M. M. Minderhoud and P. H. Bovy, "Extended time-to-collision measures for road traffic safety assessment," *Accident Anal. Prevention*, vol. 33, no. 1, pp. 89–97, Jan. 2001.
- [21] T. Streubel and K. H. Hoffmann, "Prediction of driver intended path at intersections," in *Proc. IEEE Intell. Vehicles Symp.*, Jun. 2014, pp. 134–139.
- [22] D. J. Phillips, T. A. Wheeler, and M. J. Kochenderfer, "Generalizable intention prediction of human drivers at intersections," in *Proc. IEEE Intell. Vehicles Symp. (IV)*, Jun. 2017, pp. 1665–1670.
- [23] A. Zyner, S. Worrall, J. Ward, and E. Nebot, "Long short term memory for driver intent prediction," in *Proc. IEEE Intell. Vehicles Symp. (IV)*, Jun. 2017, pp. 1484–1489.
- [24] E. Ward and J. Folkesson, "Multi-classification of driver intentions in yielding scenarios," in *Proc. IEEE 18th Int. Conf. Intell. Transp. Syst.*, Sep. 2015, pp. 678–685.

- [25] M. Quigley, K. Conley, B. Gerkey, J. Faust, T. Foote, J. Leibs, R. Wheeler, and A. Y. Ng, "ROS: An open-source robot operating system," in *Proc. ICRA Workshop Open Source Softw.*, Kobe, Japan, vol. 3, 2009, p. 5.
- [26] W. Hess, D. Kohler, H. Rapp, and D. Andor, "Real-time loop closure in 2D LIDAR SLAM," in *Proc. IEEE Int. Conf. Robot. Automat. (ICRA)*, May 2016, pp. 1271–1278.
- [27] P. Bender, J. Ziegler, and C. Stiller, "Lanelets: Efficient map representation for autonomous driving," in *Proc. IEEE Intell. Vehicles Symp.*, Jun. 2014, pp. 420–425.
- [28] F. Poggenhans, J.-H. Pauls, J. Janosovits, S. Orf, M. Naumann, F. Kuhnt, and M. Mayr, "Lanelet2: A high-definition map framework for the future of automated driving," in *Proc. IEEE Intell. Trans. Syst. Conf.*, Hawaii, HI, USA, Nov. 2018, pp. 1672–1679.
- [29] C. R. Qi, H. Su, K. Mo, and L. J. Guibas, "PointNet: Deep learning on point sets for 3D classification and segmentation," in *Proc. IEEE Conf. Comput. Vis. Pattern Recognit. (CVPR)*, Jul. 2017, pp. 652–660.
- [30] A. H. Lang, S. Vora, H. Caesar, L. Zhou, J. Yang, and O. Beijbom, "Pointpillars: Fast encoders for object detection from point clouds," in *Proc. IEEE/CVF Conf. Comput. Vis. Pattern Recognit. (CVPR)*, Jun. 2019, pp. 12697–12705.
- [31] X. Zhang, W. Xu, C. Dong, and J. M. Dolan, "Efficient L-shape fitting for vehicle detection using laser scanners," in *Proc. IEEE Intell. Vehicles Symp. (IV)*, Jun. 2017, pp. 54–59.
- [32] A. Kuznetsova, P. B. Brockhoff, and R. H. B. Christensen, "LmerTest package: Tests in linear mixed effects models," *J. Stat. Softw.*, vol. 82, no. 13, pp. 1–26, 2017.
- [33] U. Knief and W. Forstmeier, "Violating the normality assumption may be the lesser of two evils," *BioRxiv*, vol. 53, Dec. 2018, Art. no. 498931.
- [34] H. Schielzeth, N. J. Dingemans, S. Nakagawa, D. F. Westneat, H. Allegue, C. Teplitsky, D. Réale, N. A. Dochtermann, L. Z. Garamszegi, and Y. G. Araya-Ajoy, "Robustness of linear mixed-effects models to violations of distributional assumptions," *Methods Ecol. Evol.*, vol. 11, no. 9, pp. 1141–1152, 2020.
- [35] L. Breiman, "Random forests," *Mach. Learn.*, vol. 45, no. 1, pp. 5–32, 2001.
- [36] G. James, D. Witten, T. Hastie, and R. Tibshirani, *An Introduction to Statistical Learning: With Applications in R* (Springer Texts in Statistics/Springer eBook Collection), 2nd ed. New York, NY, USA: Springer, 2021.
- [37] S. M. Srinivasan, T. Truong-Huu, and M. Gurusamy, "Machine learning-based link fault identification and localization in complex networks," *IEEE Internet Things J.*, vol. 6, no. 4, pp. 6556–6566, Aug. 2019.
- [38] Y. Li, C. F. Zou, M. Bercibar, E. Elise Nanini, J. C. W. Chan, P. van den Bossche, J. Van Mierlo, and N. Omar, "Random forest regression for online capacity estimation of lithium-ion batteries," *Appl. Energy*, vol. 232, pp. 197–210, Dec. 2018.
- [39] I. Goodfellow, Y. Bengio, and A. Courville, *Deep Learning*. Cambridge, MA, USA: MIT Press, 2016. [Online]. Available: <http://www.deeplearningbook.org>



System Technologies and Image Exploitation (IOSB). His current research interests include processing of 3D data and reinforcement learning.

KEVIN QIU received the B.Sc. and M.Sc. degrees in electrical engineering and information technology from the Karlsruhe Institute of Technology (KIT), in 2018 and 2021, respectively. He contributed to this work during his Master's thesis at IIIT. He is currently pursuing the Ph.D. degree with the Fraunhofer Institute of Optronics, System Technologies and Image Exploitation (IOSB), Ettlingen, Germany. He is also a Research Associate with the Fraunhofer Institute of Optronics, System Technologies and Image Exploitation (IOSB). His current research interests include processing of 3D data and reinforcement learning.



ation Ltd. His current research interest includes the application of lidar in intelligent manufacturing.

YANCHENG JIANG received the B.Eng. degree in measurement and control technology and instrumentation from the Huazhong University of Science and Technology (HUST), China, in 2017, and the M.Sc. degree in electrical engineering and information technology from the Karlsruhe Institute of Technology (KIT), Germany in 2020. He contributed to this work during his Master's thesis at IIIT. He is currently working as a Researcher with WISDRI Engineering & Research Incorporation Ltd. His current research interest includes the application of lidar in intelligent manufacturing.



University of the Armed Forces as an Assistant Professor for Cognitive Ergonomics. In 2009, she became a Full Professor at Otto-von-Guericke-Universität Magdeburg, and in 2012, she joined the KIT. Since this time, she has been the Head of the Institute of Human and Industrial Engineering and besides, active in several committees. Her major research interests include the design of human–robot-interfaces, user state and intention prediction, and the impact of automation on human users.

BARBARA DEML studied psychology and speech communication at the University of Regensburg. Her doctoral studies were dedicated to the field of telerobotics and telepresence with a major concern on the design of haptic human-machine interaction. Her dissertation thesis in doctoral engineering was honored with a research award by the University of the Armed Forces. After postdoctoral studies at TU München and Carnegie Mellon University, Pittsburgh, PA, USA, she joined the University of the Armed Forces as an Assistant Professor for Cognitive Ergonomics. In 2009, she became a Full Professor at Otto-von-Guericke-Universität Magdeburg, and in 2012, she joined the KIT. Since this time, she has been the Head of the Institute of Human and Industrial Engineering and besides, active in several committees. Her major research interests include the design of human–robot-interfaces, user state and intention prediction, and the impact of automation on human users.



HANNES WEINREUTER received the B.Sc. and M.Sc. degrees in electrical engineering and information technology from the Karlsruhe Institute of Technology (KIT), Germany, in 2014 and 2017, respectively, where he is currently pursuing the Ph.D. degree in electrical engineering. He is also a Research Associate with the Institute of Industrial Information Technology, KIT. His current research interests include signal processing, behavior analysis, and decision-making for autonomous driving.



NADINE-REBECCA STRELAU received the B.Sc. and M.Sc. degrees in psychology from Ulm University, Germany, in 2015 and 2018, respectively. She is currently pursuing the Ph.D. degree with the Karlsruhe Institute of Technology (KIT). She is also working as a Research Associate with the Institute of Human and Industrial Engineering, KIT. Her current research interests include cooperation behavior of human drivers and the interaction of human drivers with autonomous vehicles.



From 2014 to 2016, he was a Professor in mechatronic systems with the Karlsruhe University of Applied Sciences. Since 2016, he has been a Full Professor in mechatronic measurement systems and the Director of the Institute of Industrial Information Technology, Karlsruhe Institute of Technology. His research interests include measurement and automation technology, machine vision and image processing, and image and information fusion.

MICHAEL HEIZMANN received the M.Sc. degree in mechanical engineering and the Ph.D. degree in automated visual inspection from the University of Karlsruhe, Germany, in 1998 and 2004, respectively. From 2004 to 2009, he was a Postdoctoral Research Assistant with the Fraunhofer IOSB, Karlsruhe, Germany, where he was the Head of the Department Systems for Measurement, Control and Diagnosis, from 2009 to 2016. From 2014 to 2016, he was a Professor in mechatronic systems with the Karlsruhe University of Applied Sciences. Since 2016, he has been a Full Professor in mechatronic measurement systems and the Director of the Institute of Industrial Information Technology, Karlsruhe Institute of Technology. His research interests include measurement and automation technology, machine vision and image processing, and image and information fusion.

...